Generalized slave-particle method for extended Hubbard models

Alexandru B. Georgescu[1,2] and Sohrab Ismail-Beigi[3,1,2,4]

[1]*Department of Physics, Yale University, New Haven, Connecticut 06520, USA*
[2]*Center of Research on Interface Structure and Phenomena, Yale University, New Haven, Connecticut 06520, USA*
[3]*Department of Applied Physics, Yale University, New Haven, Connecticut 06520, USA*
[4]*Department of Mechanical Engineering and Materials Science, Yale University, New Haven, Connecticut 06520, USA*

We introduce a set of generalized slave-particle models for extended Hubbard models that treat localized electronic correlations using slave-boson decompositions. Our models automatically include two slave-particle methods of recent interest, the slave-rotor and slave-spin methods, as well as a ladder of new intermediate models where one can choose which of the electronic degrees of freedom (e.g., spin or orbital labels) are treated as correlated degrees of freedom by the slave bosons. In addition, our method removes the aberrant behavior of the slave-rotor model, where it systematically overestimates the importance of electronic correlation effects for weak interaction strength, by removing the contribution of unphysical states from the bosonic Hilbert space. The flexibility of our formalism permits one to separate and isolate the effect of correlations on the key degrees of freedom.

I. INTRODUCTION

One of the long-standing areas of interest in condensed matter physics, particularly that of complex oxides, is that of the Mott metal-insulator transition [1]. Generically, within a Hubbard model framework, as the strength of localized electronic repulsions is increased, the electrons prefer to be localized on atomic sites and intersite hopping is suppressed, and at a critical interaction strength the system becomes an insulator. An example of the rich behavior that can occur in such systems is the orbital selective Mott transition (OSMT) whereby only a subset of localized orbitals become insulating (localized), while the remainder have metallic (extended) bands. An illustration is provided by the quasi-two-dimensional Mott transition in the $Ca_{2-x}Sr_xRuO_4$ family, where the Mott metal-insulator transition and its magnetic properties [2] at the critical doping $x = 0.5$ show a coexistence between a magnetic susceptibility that shows a Curie form for $S = 1/2$ and a metallic state. Anisimov *et al.* [3] have used DFT+DMFT to explain this situation in terms of an OSMT in which one Ru $4d$ orbital is localized, while the other continues to present metallic behavior.

The present day workhorse for *ab initio* materials modeling and prediction, density functional theory (DFT), is fundamentally based on band theory and is unable to describe such transitions (without symmetry breaking of the electronic degrees of freedom, e.g., spin or orbital polarization). To this end, Hubbard model based methods such as dynamical mean-field theory (DMFT) and DFT+DMFT [4,5] have been developed to include localized correlation effects in electronic structure calculations. However, DMFT-based methods are computationally expensive and typical present day calculations on real materials are generally restricted to treating a few correlated sites. Therefore it is of significant interest to have computationally inexpensive, but necessarily more approximate, methods that include correlations and can permit one to rapidly explore the qualitative effects of electronic correlations.

One set of such approximate methods that have been of recent interest are slave-particle methods. Slave-boson methods have a long background in condensed matter theory for analytical treatments of correlations typically in the limiting case of infinite correlation strength [6–12]. Kotliar and Ruckenstein [11] used a slave-particle representation to treat Hubbard-like models at finite interaction strength, which found applications in the realm of high-temperature superconductivity [13]. Further, Kotliar and Ruckenstein's model has been generalized to multiband models [14–16] where, e.g., the effects of multiple orbitals, orbital degeneracy, and the Hund's interaction have been studied [14,15]. However, the approach of Kotliar and Ruckenstein, and its various extensions, require a large number of bosonic slave particles: one needs one boson per possible electronic configuration on a correlated site.

For this reason, more economical slave-boson representations have been of significant interest. Florens and Georges [17,18] used a single "rotor" slave-boson per site that describes the total electron count on each site in a computationally economical manner. The slave-rotor method successfully predicted a number of electronic phases of nickelate heterostructures [19], which was a distinct improvement over previous studies. However, a rotorlike description is not orbitally selective as it can only describe the total electron count on a site and not its partitioning among inequivalent orbitals on that site. An alternative slave-particle approach is to treat each localized electronic state (i.e., a unique combination of spin and orbital indices) with a slave boson: this "slave-spin" approach automatically handles orbital symmetry breaking and can predict OSMTs [20,21]. Recently, it has been applied to predict key physical characteristics in iron superconductors [22].

In this work, we introduce a generalized framework for slave-particle descriptions. This produces a ladder of correlated models, and the slave-rotor and slave-spin are automatically included as two specific cases. Our approach does not require any physical analogies to create the slave bosons (e.g., a quantum rotor or angular variable to motivate the slave rotor or a pseudospin to motive the slave spin) and works directly in the occupation number representation. In our approach, one can choose which degrees of freedom are

treated as correlated degrees of freedom (e.g., total electron count on a site, electron counts in each orbital, electron count in each spin channel, etc.) so that we can isolate the effect of correlations on the separate degrees of freedom in a systematic manner. Section II presents our general formalism, how it builds upon previous models, as well as gives a few examples of models that can be built within this framework. Section III is devoted to tests of possible models built within this formalism in a mean-field approach at half-filling within a one-band and a two-band model in order to compare our results with those of previous work as well as to better understand the role of the different terms in an extended Hubbard model within our formalism. In Sec. IV, we conclude this paper and discuss possible avenues for researchers to use this method and possible developments of it in predicting properties of correlated materials.

II. THE GENERALIZED SLAVE-PARTICLE REPRESENTATION

In this section, we introduce our generalized slave-particle representation. In appropriate limits, our approach reproduces previous frameworks such as the slave-rotor and slave-spin methods. One utility of our approach is that it allows us to unite these two, as well as other intermediate models, into a single slave-particle methodology. A variety of slave-particle models can be investigated and compared so that one can isolate which specific correlated degrees of freedom are critical for describing a specific physical problem.

A. Extended Hubbard model

The general correlated-electron Hamiltonian we consider is an extended Hubbard model given by

$$\hat{H} = \sum_i \hat{H}^i_{\text{int}} + \sum_{im\sigma} \epsilon_{im\sigma} \hat{d}^\dagger_{im\sigma} \hat{d}_{im\sigma}$$
$$- \sum_{ii'mm'\sigma} t_{imi'm'\sigma} \hat{d}^\dagger_{im\sigma} \hat{d}_{i'm'\sigma}. \tag{1}$$

The index i ranges over the localized sites of the system (usually atomic sites), m ranges over the localized spatial orbitals on each site, σ denotes spin, $\hat{H}^i_{\text{int}}$ is the local Coulombic interaction for site i detailed further below, $\epsilon_{im\sigma}$ is the onside energy of the orbital $im\sigma$, and $t_{imi'm'\sigma}$ is the spin-conserving hopping element connecting orbital $im\sigma$ to $i'm'\sigma$. The $\hat{d}$ are canonical fermion annihilation operators. We take the interaction term to have the standard Slater-Kanamori form [23]

$$\hat{H}^i_{\text{int}} = \frac{U_i}{2}\big(\hat{n}_i^2 - \hat{n}_i\big) + \frac{U'_i - U_i}{2} \sum_{m\neq m'} \hat{n}_{im}\hat{n}_{im'}$$
$$- \frac{J_i}{2} \sum_\sigma \sum_{m\neq m'} \hat{n}_{im\sigma}\hat{n}_{im'\sigma}$$
$$- \frac{J_i}{2} \sum_\sigma \sum_{m\neq m'} (\hat{d}^\dagger_{im\sigma}\hat{d}_{im\bar\sigma}\hat{d}^\dagger_{im'\bar\sigma}\hat{d}_{im'\sigma}$$
$$+ \hat{d}^\dagger_{im\sigma}\hat{d}^\dagger_{im\bar\sigma}\hat{d}_{im'\sigma}\hat{d}_{im'\bar\sigma}). \tag{2}$$

The first and second term stem from Coulombic repulsion terms between the same spatial orbital (U) and different spatial orbitals (U'). The third term is Hund's exchange between different orbitals of the same spin with strength J. The fourth term contains the intrasite "spin-flip" and "pair-hopping" terms. The index $\bar\sigma$ is the spin opposite to σ. The subscripts i on the U, U', and J parameters denote the fact that each correlated site can have its own set of parameters; however, to keep indices to a minimum below, we suppress this index. The various number operators are

$$\hat{n}_{im\sigma} = \hat{d}^\dagger_{im\sigma}\hat{d}_{im\sigma}, \qquad \hat{n}_{im} = \sum_\sigma \hat{n}_{im\sigma},$$

$$\hat{n}_{i\sigma} = \sum_m \hat{n}_{im\sigma}, \qquad \hat{n}_i = \sum_{m\sigma} \hat{n}_{im\sigma}.$$

For what follows, we keep in mind that due to the fact that $\hat{n}^2_{im\sigma} = \hat{n}_{im\sigma}$, the Hund's term in $\hat{H}^i_{\text{int}}$ can be rewritten in an equivalent form to give

$$\hat{H}^i_{\text{int}} = \frac{U_i}{2}\big(\hat{n}_i^2 - \hat{n}_i\big) + \frac{U'_i - U_i}{2} \sum_{m\neq m'} \hat{n}_{im}\hat{n}_{im'}$$
$$- \frac{J_i}{2} \sum_\sigma \big(\hat{n}^2_{i\sigma} - \hat{n}_{i\sigma}\big)^2$$
$$- \frac{J_i}{2} \sum_\sigma \sum_{m\neq m'} (\hat{d}^\dagger_{im\sigma}\hat{d}_{im\bar\sigma}\hat{d}^\dagger_{im'\bar\sigma}\hat{d}_{im'\sigma}$$
$$+ \hat{d}^\dagger_{im\sigma}\hat{d}^\dagger_{im\bar\sigma}\hat{d}_{im'\sigma}\hat{d}_{im'\bar\sigma}). \tag{}$$

B. Spinons and slave bosons

The interacting Hubbard Hamiltonian is impossible to solve exactly and even difficult to solve approximately. Part of the difficulty comes from the fact that we have interacting fermions which have both charge and spin degrees of freedom. Following well-known ideas in slave-boson approaches [6–12], one separates at each site the fermionic degrees of freedom from the charge degrees of freedom by introducing a bosonic "slave" particle on that site. The boson is spinless and charged, and one also has a remaining neutral fermion with spin termed a spinon.

With spinons denoted by $\hat{f}$ operators and slave bosons by $\hat{O}$ operators, we define

$$\hat{d}_{im\sigma} = \hat{f}_{im\sigma}\hat{O}_{i\alpha} \tag{3}$$

and

$$\hat{d}^\dagger_{im\sigma} = \hat{f}^\dagger_{im\sigma}\hat{O}^\dagger_{i\alpha}. \tag{4}$$

Requiring the $\hat{f}$ to be fermionic field operators in turn requires the $\hat{O}$ operators to obey bosonic commutation relations. We note that while the $\hat{f}$ spinon operators are standard fermionic Fock field operators, the bosonic $\hat{O}$ operators are generic and *ad hoc*: there is no assumption or requirement that the $\hat{O}$ be bosonic operators for a Fock space (and in general they are not of that variety).

The index α is part of our generalized notation that permits us to unify many slave-particle models. The meaning of α depends on the type of model chosen, as we will show in detail below with a variety of examples. The index α refers

to a subset of the complete set of $m\sigma$ indices that belong to a site i. For example, if we use an O(2) slave-rotor model for the correlated orbitals on an site [17,18] where $\hat{O} = e^{-i\hat{\theta}}$ and θ is the phase angle of the O(2) rotor, then α is nil: $\hat{O}_{i\alpha} = \hat{O}_i$. Namely, we have a single slave particle on each site i that tracks the total number of particles on that site. At the opposite limit, we can have a unique slave boson for each $m\sigma$ (the "slave-spin" method [20,21]), so that $\alpha = m\sigma$.

We work directly in the number representation and introduce a number operator for the slave particles (this is a generalization of the angular momentum operator for the slave-rotor approach or the $S_z^{im\sigma}$ quasispin of the slave-spin representation). The minimum and maximum allowed particle numbers are $N_{\min}$ and $N_{\max}$ so that

$$\hat{N}_{i\alpha} = \text{diag}\,(N_{\min}, N_{\min} + 1, \ldots, N_{\max} - 1, N_{\max}). \quad (5)$$

This operator simply keeps track of the number of slave particles in each slave mode $i\alpha$, and the minimum and maximum allowed occupancies depends the slave model we choose as discussed below.

Since we have introduced new degrees of freedom and enlarged the Hilbert space of the problem, it is necessary to enforce constraints so that one avoids considering "unphysical states" that have no correspondence to those in the original problem. The original Hilbert space is spanned by kets of the form $|\{n_{im\sigma}\}\rangle$ in the occupancy basis of the $\hat{d}_{im\sigma}$ operators. The enlarged Hilbert space is spanned by kets of the product form $|\{n_{im\sigma}\}\rangle_f |\{N_{i\alpha}\}\rangle_s$ where the subscripts label spinon and slave sectors. Within this enlarged space, there is a subset of "physical states" that correspond to the original kets. The first part of the correspondence is make the fermionic occupancies $\{n_{im\sigma}\}$ of the original electron counts ($\hat{d}$) and the spinon counts ($\hat{f}$) identical. Hence, the real question is which $N_{i\alpha}$ are physically allowed.

Equations (3) and (4) mean that the number of spinon and slave particles on each site must track each other because they are annihilated and created at the same time. Hence, following ideas from prior work [17,20], we enforce constraints to ensure the particle numbers track each other. We enforce the constraint

$$\sum_{m\sigma \in \alpha} \hat{f}_{im\sigma}^\dagger \hat{f}_{im\sigma} |\phi\rangle = \hat{N}_{i\alpha} |\phi\rangle \quad (6)$$

on the kets $|\phi\rangle$ in the enlarged space. Only these kets are physically allowed in the exact description of the system, and they span the physical subspace. We note that the constraint is on the allowed kets and not on the operators: the operators act in the extended Hilbert space that includes physical and unphysical unphysical states, and the $\hat{f}$ or $\hat{O}$ operators acting alone can move us from a physical state to an unphysical state.

Enforcing the constraints of Eq. (6) ensures that only physical states that are in one-to-one correspondence to the original states are considered in the extended spinon+slave-boson Hilbert space. (This is the same idea as Ref. [17] where the O(2) rotor angular momentum operator $\hat{L}$ has been replaced by $\hat{N}_{i\alpha}$.) When the constraints are obeyed, only physically allowed occupancies for the bosonic operators are relevant which is the same as setting $N_{\min} = 0$ and $N_{\max}$ to the maximum allowed occupancy in the slave sector on the site. For example, for a system of three spatial orbitals on a site

(i.e., three choices of m), $N_{\max} = 6$ if we only wish to count total numbers of electrons using the slave bosons in which case α is nil. Or, if we want to count up and down spin electrons separately for this site, then α is the same as σ and $N_{\max} = 3$ for each choice of α. However, as explained below, when one does approximate calculations, choosing $N_{\min}$ and $N_{\max}$ that differ from these values allows for the creation of different types of models and offers some technical advantages.

For completeness and clarity, the Appendix provides explicit examples of the enlarged Hilbert spaces and various choices of α and explains how the action of the $\hat{d}_{im\sigma}$ and the $\hat{f}_{im\sigma} \hat{O}_{i\alpha}$ operators are identical on the physical subspace of states.

C. Slave operators and Hamiltonian

To reproduce the standard behavior of the annihilation operator where only physical states are allowed in the spectrum of the operator [20,21] (also see the Appendix),

$$\hat{d}_{im\sigma} |n_{im\sigma}\rangle = \sqrt{n_{im\sigma}} |n_{im\sigma} - 1\rangle, \quad (7)$$

it must be that

$$\hat{f}_{im\sigma} |n_{im\sigma}\rangle_f = \sqrt{n_{im\sigma}} |n_{im\sigma} - 1\rangle_f \quad (8)$$

and

$$\hat{O}_{i\alpha} |N_{i\alpha}\rangle_s = |N_{i\alpha} - 1\rangle_s. \quad (9)$$

However, if $n_{im\sigma} = 0$, then the action of $\hat{f}_{im\sigma}$ will destroy the total state $|\phi\rangle$ regardless of what $\hat{O}_\alpha$ may do, so for this case we have an undetermined situation:

$$\hat{O}_{i\alpha} |N_{i\alpha} = 0\rangle_s = \text{undetermined}. \quad (10)$$

Following the same logic for the creation operators yields

$$\hat{O}_{i\alpha}^\dagger |N_{i\alpha}\rangle_s = |N_{i\alpha} + 1\rangle_s \quad (11)$$

until we reach the ceiling $N_{i\alpha} = N_{\max}$ when we have a similar indeterminacy

$$\hat{O}_{i\alpha}^\dagger |N_{\max}\rangle_s = \text{undetermined}.$$

Putting this all together, the slave-boson operator $\hat{O}_{i\alpha}$ in the number basis must have the form

$$\hat{O}_{i\alpha} = \begin{pmatrix} 0 & 1 & 0 & \ldots & 0 & 0 \\ 0 & 0 & 1 & \ldots & 0 & 0 \\ \vdots & \vdots & \vdots & \ddots & \vdots & \vdots \\ 0 & 0 & 0 & \ldots & 1 & 0 \\ 0 & 0 & 0 & \ldots & 0 & 1 \\ C_{i\alpha} & 0 & 0 & \ldots & 0 & 0 \end{pmatrix}, \quad (12)$$

where $C_{i\alpha}$ is at this point an undetermined constant that we are free to choose. Below, we will use this freedom to ensure that we reproduce a desired noninteracting band structure at zero interaction strength (when $\hat{H}_{\text{int}}^i = 0$).

Substituting the spinon and slave operators into the original extended Hubbard Hamiltonian gives the following form, which for the moment we specialize to the symmetric $U' = U, J = 0$ case to keep the logic simple (the more general cases

are enumerated further below):

$$
\hat{H} = \frac{U}{2} \sum_i \left[\left(\sum_\alpha \hat{N}_{i\alpha} \right)^2 - \sum_\alpha \hat{N}_{i\alpha} \right]
$$
$$
+ \sum_{im\sigma} \epsilon_{im\sigma} \hat{f}^\dagger_{im\sigma} \hat{f}_{im\sigma}
$$
$$
- \sum_{ii'mm'\sigma} t_{imi'm'\sigma} \hat{O}^\dagger_{i\alpha} \hat{O}_{i'\alpha'} \hat{f}^\dagger_{im\sigma} \hat{f}_{i'm'\sigma}.
$$

For the onsite $\epsilon_{im\sigma}$ terms, we have replaced $\hat{f}^\dagger_{im\sigma} \hat{f}_{im\sigma} \hat{O}^\dagger_{i\alpha} \hat{O}_{i\alpha}$ by the simpler $\hat{f}^\dagger_{im\sigma} \hat{f}_{im\sigma}$ because even though $\hat{O}^\dagger_{i\alpha} \hat{O}_{i\alpha}$ is not necessarily identity (unless $C_{i\alpha} = 1$), the two set of operators act identically on all the physical states of interest due to the fact that $\hat{f}_{im\sigma}$ annihilates the state with zero particles.

The point of introducing the slave degree of freedom is that they track the number of electrons in the various orbitals and spin states on each site *and* the interaction Hamiltonian of Eq. (2) is essentially determined by these numbers. Hence, one can write the most important parts of the interaction Hamiltonian solely in terms of the bosonic slave operators.

D. Decoupling spinons and slaves

Up to this point, our considerations have been for an exact solution of the interacting Hamiltonian which is impossible in practice. To make progress, in slave-particle approaches one splits the problem into two separate and simpler pieces that are connected to each other via self-consistent averages of the relevant operators. Specifically, the ground-state wave function of the system is approximated by a simple, separable product state $|\Psi_f\rangle |\Phi_s\rangle$ where $|\Psi_F\rangle$ is a spinon wave function and $|\Phi_s\rangle$ is a slave-boson wave function. Since the spinons and slaves are now decoupled and their number fluctuations are no longer locked in step, the constraint of Eq. (6) can only be satisfied on average,

$$
\left\langle \sum_{m\sigma \in \alpha} \hat{f}^\dagger_{im\sigma} \hat{f}_{im\sigma} \right\rangle_f = \langle \hat{N}_{i\alpha} \rangle_s, \tag{13}
$$

where the f and s subscripts denote averaging over the spinon $|\Psi_f\rangle$ and slave-boson $|\Phi_s\rangle$ ground-state wave functions, respectively.

A priori, one can make only few statements about when such a decoupling scheme is expected to be a good approximation. First, at zero interaction strength ($U = J = 0$), the decoupled approach can reproduce the noninteracting band structure since the spinons alone can do this. Second, if number fluctuations about the averages are small so that imposing Eq. (13) is close to imposing Eq. (6), then we expect the decoupling to work well in describing ground-state averages; examples of phases with small or zero number fluctuations are narrow or Mott-like insulating bands. Third, in infinite dimensions as well as in one dimension, due to the similarity of the main equations (see below) with the Gutzwiller approximation [16,18,20,24], one can say the two approaches should succeed or fail together. Unfortunately, in two or three dimensions—which are cases of common interest—there is no *a priori* way to know whether the approximation will be good or poor.

We note that when the decoupling approximation is performed and the constraint imposed only on average in Eq. (13), we may decide to change $N_{\min}$ and $N_{\max}$ to allow additional unphysical states with negative or positive occupations. For example, letting $N_{\min} \to -\infty$ and $N_{\max} \to +\infty$, which in turn makes $C_{i\alpha}$ irrelevant, yields the mean-field O(2) slave-rotor formalism used in previous work [17,18]. As noted previously [20], allowing these unphysical states is not a major error in the limit of strong interactions since number fluctuations to unphysical occupancies are at any rate unlikely due to their large Coulombic penalties; however, for small interaction strengths, the unphysical states have significant weight in the wave function which creates incorrect behavior, e.g., improper behavior of the quasiparticle weight versus interaction strength. At the other extreme, a separate slave boson for each spin+orbital combination $im\sigma$ gives $N_{\min} = 0$ and $N_{\max} = 1$, which is just the "slave-spin" formalism [20,21].

With this separability assumption, the time-independent Schrödinger equation for the original system separates into two separate equations where the constraints of Eq. (13) are enforced by Lagrange multipliers $h_{i\alpha}$ appearing in the two Hamiltonians. In the remainder of this section, we discuss the simplest $U = U'$ and $J = 0$ case for simplicity. Full expressions involving U, U', and J for various slave-boson choices follow after this section. The spinon Hamiltonian is

$$
\hat{H}_f = \sum_{im\sigma} \epsilon_{im\sigma} \hat{f}^\dagger_{im\sigma} \hat{f}_{im\sigma} - \sum_{i\alpha} h_{i\alpha} \sum_{m\sigma \in \alpha} \hat{f}^\dagger_{im\sigma} \hat{f}_{im\sigma}
$$
$$
- \sum_{ii'\alpha\alpha'} \langle \hat{O}^\dagger_{i\alpha} \hat{O}_{i'\alpha'} \rangle_s \sum_{\substack{m\sigma \in \alpha \\ m'\sigma \in \alpha'}} t_{imi'm'\sigma} \hat{f}^\dagger_{im\sigma} \hat{f}_{i'm'\sigma}. \tag{14}
$$

The spinons are coupled to the slave bosons via the average $\langle \hat{O}^\dagger_{i\alpha} \hat{O}_{i'\alpha'} \rangle_s$, which renormalizes spinon hoppings between sites i and i'. The spinon problem is one of noninteracting fermionic particles with spin.

The slave-boson Hamiltonian takes the form

$$
\hat{H}_s = \frac{U}{2} \sum_i \left[\left(\sum_\alpha \hat{N}_{i\alpha} \right)^2 - \sum_\alpha \hat{N}_{i\alpha} \right] + \sum_\alpha h_{i\alpha} \hat{N}_{i\alpha}
$$
$$
- \sum_{ii'\alpha\alpha'} \left(\sum_{\substack{m\sigma \in \alpha \\ m'\sigma \in \alpha'}} t_{imi'm'\sigma} \langle \hat{f}^\dagger_{im\sigma} \hat{f}_{i'm'\sigma} \rangle_f \right) \hat{O}^\dagger_{i\alpha} \hat{O}_{i'\alpha'} \tag{15}
$$

where the spinon average $\langle \hat{f}^\dagger_{im\sigma} \hat{f}_{i'm'\sigma} \rangle_f$ renormalizes the slave-boson hoppings. The slave-boson problem is one of interacting charged bosons without spin.

The original problem has been reduced to a set of paired problems that must be solved self-consistently. The spinon and slave-boson problems only communicate (i.e., are coupled) via averages which renormalize each other's hoppings. At this point, one must make some approximations in order to solve the interacting bosonic problem. Typical approaches to date include single-site mean-field approximations [17,18], multiple-site mean-field [25], approximation by sigma models to yield Gaussian integrals [17,18] as well as a combination

of using tight-binding parameters obtained using Wannier functions from DFT followed by a mean-field approximation [19].

Separately, a procedure is needed to obtain the $C_{i\alpha}$. To this end, at $U = U' = J = 0$, one chooses the $C_{i\alpha}$ to ensure that the spinon bands reproduce the original noninteracting band structure and associated occupancies (i.e., fillings). This means that the slave-boson expectations $\langle \hat{O}_{i\alpha}^\dagger \hat{O}_{i'\alpha'} \rangle_s$ should be unity in order not to modify the spinon hoppings away from the original noninteracting hoppings $t_{imi'm'\sigma}$. The numbers $C_{i\alpha}$ and $h_{i\alpha}$ are determined by making $\langle \hat{O}_{i\alpha}^\dagger \hat{O}_{i'\alpha'} \rangle_s$ unity as well as reproducing the noninteracting occupancies or fillings. This actually requires us to solve the coupled slave and spinon problems at $U = U' = J = 0$ self-consistently to obtain $C_{i\alpha}$ and $h_{i\alpha}$. The values of $C_{i\alpha}$ are then held fixed from that point forth when turning on U, U', J to nonzero values to self-consistently solve the actual interacting problem.

Prior to solving some model problems within our new framework, we provide more complete descriptions of a number of potential choices for the slave-boson model (i.e., the choice of α) with full U, U', and J dependence. Differing choices split the interaction terms $\hat{H}_{\rm int}^i$ of Eq. (2) in different ways between the spinon and slave sectors. This opens the door to systematic comparison between the different types of treatments of correlations with the slave bosons.

1. Number slave

The simplest approach is to simply create a single slave boson on each site i whose number operator $\hat{N}_i$ counts all the electrons on that site. In other words, the label α contains all the $m\sigma$ orbitals on that site: it is superfluous so we can write $\hat{O}_{i\alpha} = \hat{O}_i$. Description of the physically allowed states will set $N_{\rm min} = 0$ while $N_{\rm max}$ will be the maximum number of electrons allowed on that site, e.g., 10 for d shells or 14 for f shells.

In this case, the slave boson can only represent the U term of the interaction in Eq. (2); all remaining interaction terms must be treated at the mean-field level in the spinon sector. The slave Hamiltonian in this case is

$$\hat{H}_s = \frac{U}{2} \sum_i \left(\hat{N}_i^2 - \hat{N}_i \right) + \sum_i h_i \hat{N}_i$$
$$- \sum_{ii'} \left(\sum_{mm'\sigma} t_{imi'm'\sigma} \langle \hat{f}_{im\sigma}^\dagger \hat{f}_{i'm'\sigma} \rangle_f \right) \hat{O}_i^\dagger \hat{O}_{i'}, \quad (16)$$

while the spinon Hamiltonian contains all the remaining interaction terms at mean-field level:

$$\hat{H}_f = \frac{U'-U}{2} \sum_i \sum_{m \neq m'} \left[n_{im}\hat{n}_{im'} + n_{im'}\hat{n}_{im} - \sum_{\sigma\sigma'} (\rho_{im'\sigma'im\sigma} \hat{f}_{im'\sigma'}^\dagger \hat{f}_{im\sigma} + \rho_{im\sigma im'\sigma'} \hat{f}_{im\sigma}^\dagger \hat{f}_{im'\sigma'}) \right]$$
$$- \frac{J}{2} \sum_{i\sigma} \sum_{m \neq m'} (n_{im\sigma}\hat{n}_{im'\sigma} + n_{im'\sigma}\hat{n}_{im\sigma} - \rho_{im'\sigma'im\sigma} \hat{f}_{im'\sigma'}^\dagger \hat{f}_{im\sigma} - \rho_{im\sigma im'\sigma'} \hat{f}_{im\sigma}^\dagger \hat{f}_{im'\sigma'})$$
$$- \frac{J}{2} \sum_{i\sigma} \sum_{m \neq m'} (\rho_{im\bar{\sigma}im\sigma} \hat{f}_{im'\bar{\sigma}}^\dagger \hat{f}_{im'\sigma} + \rho_{im'\sigma im\bar{\sigma}} \hat{f}_{im\sigma}^\dagger \hat{f}_{im\bar{\sigma}} - \rho_{im\sigma im\sigma} \hat{f}_{im'\bar{\sigma}}^\dagger \hat{f}_{im\bar{\sigma}} - \rho_{im\bar{\sigma}im'\sigma} \hat{f}_{im\sigma}^\dagger \hat{f}_{im'\sigma}$$
$$+ \rho_{im'\bar{\sigma}im\sigma} \hat{f}_{im\bar{\sigma}}^\dagger \hat{f}_{im'\sigma} + \rho_{im'\sigma im\sigma} \hat{f}_{im\sigma}^\dagger \hat{f}_{im'\bar{\sigma}} - \rho_{im'\sigma im\sigma} \hat{f}_{im\bar{\sigma}}^\dagger \hat{f}_{im'\bar{\sigma}} - \rho_{im'\bar{\sigma}im\sigma} \hat{f}_{im\sigma}^\dagger \hat{f}_{im'\sigma})$$
$$+ \sum_{im\sigma} \epsilon_{im\sigma} \hat{f}_{im\sigma}^\dagger \hat{f}_{im\sigma} - \sum_i h_i \hat{n}_i - \sum_{ii'} \langle \hat{O}_i^\dagger \hat{O}_{i'} \rangle_s \sum_{mm'\sigma} t_{imi'm'\sigma} \hat{f}_{im\sigma}^\dagger \hat{f}_{i'm'\sigma}. \quad (17)$$

In the derivation of the expression for the above spinon Hamiltonian $\hat{H}_f$, we have used the definition of the one-particle density matrix

$$\rho_{ba} = \langle \hat{f}_a^\dagger \hat{f}_b \rangle_f,$$

the standard mean-field contraction of four-particle operators into two-particle operators weighed by averages

$$\hat{f}_a^\dagger \hat{f}_b^\dagger \hat{f}_c \hat{f}_d \approx \rho_{da} \hat{f}_b^\dagger \hat{f}_c - \rho_{ca} \hat{f}_b^\dagger \hat{f}_d + \rho_{cb} \hat{f}_a^\dagger \hat{f}_d - \rho_{db} \hat{f}_a^\dagger \hat{f}_c,$$

and the average occupations

$$n_{im\sigma} = \rho_{im\sigma im\sigma}, \quad n_{im} = \sum_\sigma n_{im\sigma}.$$

This approach has the simplest slave Hamiltonian and the most complex spinon Hamiltonian. This is because the number-only slave boson can only describe the simplest U part of the interaction; the remaining terms involving U' and J must

be handled at mean-field level by the spinons. As mentioned above, the physical range for the occupation numbers of the number slave $\hat{N}_i$ is from zero to the physically allowed $N_{\rm max}$ for that site. However, we can decrease $N_{\rm min}$ below zero and $N_{\rm max}$ above the physical value if desired: in the limit where the range of occupancies allowed is very large, we automatically recover the O(2) slave-rotor method.

2. Orbital slave

A more fine-grained model is to count the number of electrons in each spatial orbital m separately with a slave boson. We call this the orbital slave method. Here, the index α labels a specific spatial orbital m and ranges over the two spin directions for that orbital: we have $\hat{O}_{im}$ for the raising/lowering operator and $\hat{N}_{im}$ for the particle count slave operators. The slave sector can now directly describe more of the interaction

terms:

$$\hat{H}_s = \frac{U}{2}\sum_i\left[\left(\sum_m\hat{N}_{im}\right)^2 - \sum_m\hat{N}_{im}\right] + \frac{U'-U}{2}\sum_i\sum_{m\neq m'}\hat{N}_{im}\hat{N}_{im'}$$

$$+ \sum_i\sum_m h_{im}\hat{N}_{im} - \sum_{ii'mm'}\left(\sum_\sigma t_{imi'm'\sigma}\langle\hat{f}^\dagger_{im\sigma}\hat{f}_{i'm'\sigma}\rangle_f\right)\hat{O}^\dagger_{im}\hat{O}_{i'm'} \tag{18}$$

and the spinon Hamiltonian is less complex than the previous case as it only has the J terms at mean-field level:

$$\hat{H}_f = -\frac{J}{2}\sum_{i\sigma}\sum_{m\neq m'}(n_{im\sigma}\hat{n}_{im'\sigma} + n_{im'\sigma}\hat{n}_{im\sigma} - \rho_{im'\sigma'im\sigma}\hat{f}^\dagger_{im'\sigma'}\hat{f}_{im\sigma} - \rho_{im\sigma im'\sigma'}\hat{f}^\dagger_{im\sigma}\hat{f}_{im'\sigma'})$$

$$-\frac{J}{2}\sum_{i\sigma}\sum_{m\neq m'}(\rho_{im\bar\sigma im\sigma}\hat{f}^\dagger_{im'\bar\sigma}\hat{f}_{im'\sigma} + \rho_{im'\sigma im'\bar\sigma}\hat{f}^\dagger_{im\sigma}\hat{f}_{im\bar\sigma} - \rho_{im'\sigma im\sigma}\hat{f}^\dagger_{im'\bar\sigma}\hat{f}_{im\bar\sigma} - \rho_{im\bar\sigma im'\bar\sigma}\hat{f}^\dagger_{im\sigma}\hat{f}_{im'\sigma} + \rho_{im'\bar\sigma im\sigma}\hat{f}^\dagger_{im\bar\sigma}\hat{f}_{im'\sigma}$$

$$+ \rho_{im'\bar\sigma im\bar\sigma}\hat{f}^\dagger_{im\sigma}\hat{f}_{im'\sigma} - \rho_{im'\sigma im\sigma}\hat{f}^\dagger_{im\bar\sigma}\hat{f}_{im'\bar\sigma} - \rho_{im\bar\sigma im'\bar\sigma}\hat{f}^\dagger_{im\sigma}\hat{f}_{im'\sigma})$$

$$+ \sum_{im\sigma}\epsilon_{im\sigma}\hat{f}^\dagger_{im\sigma}\hat{f}_{im\sigma} - \sum_i\sum_m h_{im}\hat{n}_{im} - \sum_{ii'mm'}\langle\hat{O}^\dagger_{im}\hat{O}_{i'm'}\rangle_s\sum_\sigma t_{imi'm'\sigma}\hat{f}^\dagger_{im\sigma}\hat{f}_{i'm'\sigma}. \tag{19}$$

3. Spin slave

An alternative fine-graining is to have two slave bosons per site that count spin-up and spin-down electrons separately but with no orbital differentiation. Namely, α labels a spin state σ but ranges over all spatial orbitals. Hence we have $\hat{O}_{i\sigma}$ and $\hat{N}_{i\sigma}$ for our slave operators. The slave-boson Hamiltonian is

$$\hat{H}_s = \frac{U}{2}\sum_i\left[\left(\sum_\sigma\hat{N}_{i\sigma}\right)^2 - \sum_\sigma\hat{N}_{i\sigma}\right] - \frac{J}{2}\sum_\sigma(\hat{N}^2_{i\sigma} - \hat{N}_{i\sigma}) + \sum_i\sum_\sigma h_{i\sigma}\hat{N}_{i\sigma} - \sum_{ii'\sigma}\left(\sum_{mm'}t_{imi'm'\sigma}\langle\hat{f}^\dagger_{im\sigma}\hat{f}_{i'm'\sigma}\rangle_f\right)\hat{O}^\dagger_{i\sigma}\hat{O}_{i'\sigma}, \tag{20}$$

while the spinon Hamiltonian is

$$\hat{H}_f = \frac{U'-U}{2}\sum_i\sum_{m\neq m'}\left[n_{im}\hat{n}_{im'} + n_{im'}\hat{n}_{im} - \sum_{\sigma\sigma'}(\rho_{im'\sigma'im\sigma}\hat{f}^\dagger_{im'\sigma'}\hat{f}_{im\sigma} + \rho_{im\sigma im'\sigma'}\hat{f}^\dagger_{im\sigma}\hat{f}_{im'\sigma'})\right]$$

$$-\frac{J}{2}\sum_{i\sigma}\sum_{m\neq m'}(\rho_{im\bar\sigma im\sigma}\hat{f}^\dagger_{im'\bar\sigma}\hat{f}_{im'\sigma} + \rho_{im'\sigma im'\bar\sigma}\hat{f}^\dagger_{im\sigma}\hat{f}_{im\bar\sigma} - \rho_{im'\sigma im\sigma}\hat{f}^\dagger_{im'\bar\sigma}\hat{f}_{im\bar\sigma} - \rho_{im\bar\sigma im'\bar\sigma}\hat{f}^\dagger_{im\sigma}\hat{f}_{im'\sigma} + \rho_{im'\bar\sigma im\sigma}\hat{f}^\dagger_{im\bar\sigma}\hat{f}_{im'\sigma}$$

$$+ \rho_{im'\sigma im\bar\sigma}\hat{f}^\dagger_{im\sigma}\hat{f}_{im'\bar\sigma} - \rho_{im'\sigma im\sigma}\hat{f}^\dagger_{im\bar\sigma}\hat{f}_{im'\bar\sigma} - \rho_{im\bar\sigma im'\bar\sigma}\hat{f}^\dagger_{im\sigma}\hat{f}_{im'\sigma})$$

$$+ \sum_{im\sigma}\epsilon_{im\sigma}\hat{f}^\dagger_{im\sigma}\hat{f}_{im\sigma} - \sum_i\sum_m h_{im}\hat{n}_{im} - \sum_{ii'mm'}\langle\hat{O}^\dagger_{im}\hat{O}_{i'm'}\rangle_s\sum_\sigma t_{imi'm'\sigma}\hat{f}^\dagger_{im\sigma}\hat{f}_{i'm'\sigma}. \tag{21}$$

4. Spin+orbital slave

This approach represents maximum fine-graining whereby we use a slave boson for each spin+orbital combination. Thus the index α now represents a full set of quantum numbers $m\sigma$ so we have $\hat{O}_{im\sigma}$ and $\hat{N}_{im\sigma}$ for the slave operators. The physically allowed occupancies are 0 and 1 which is isomorphic to a pseudospin. For this reason, the name used for this approach in the literature is the "slave-spin" method [20,21]. However, given the possible confusion this term creates between the real electron spin as well as the difficulty of using such a name unambiguously in our generalized formalism, we prefer the more explicit name "spin+orbital-slave" where the spin refers to the physical electron spin.

In this approach, we can describe the maximum number of interaction terms in the slave Hamiltonian:

$$\hat{H}_s = \frac{U}{2}\sum_i\left[\left(\sum_{m\sigma}\hat{N}_{im\sigma}\right)^2 - \sum_{m\sigma}\hat{N}_{im\sigma}\right] + \frac{U'-U}{2}\sum_{m\neq m'}\left(\sum_\sigma\hat{N}_{im\sigma}\right)\left(\sum_{\sigma'}\hat{N}_{im'\sigma'}\right) - \frac{J}{2}\sum_\sigma\sum_{m\neq m'}\hat{N}_{im\sigma}\hat{N}_{im'\sigma}$$

$$+ \sum_i\sum_{m\sigma} h_{im\sigma}\hat{N}_{im\sigma} - \sum_{ii'mm'\sigma} t_{imi'm'\sigma}\langle\hat{f}^\dagger_{im\sigma}\hat{f}_{i'm'\sigma}\rangle_f\hat{O}^\dagger_{im\sigma}\hat{O}_{i'm'\sigma}. \tag{22}$$

The corresponding spinon Hamiltonian still contains the spin-flip and pair-hopping terms:

$$
\hat{H}_f = -\frac{J}{2} \sum_{i\sigma} \sum_{m \neq m'} (\rho_{im\bar{\sigma}im\sigma} \hat{f}^\dagger_{im'\bar{\sigma}} \hat{f}_{im'\sigma} + \rho_{im'\sigma im'\bar{\sigma}} \hat{f}^\dagger_{im\sigma} \hat{f}_{im\bar{\sigma}} - \rho_{im'\sigma im\sigma} \hat{f}^\dagger_{im\bar{\sigma}} \hat{f}_{im'\sigma} - \rho_{im\bar{\sigma}im'\bar{\sigma}} \hat{f}^\dagger_{im\sigma} \hat{f}_{im'\sigma} + \rho_{im'\bar{\sigma}im\sigma} \hat{f}^\dagger_{im\bar{\sigma}} \hat{f}_{im'\sigma}
$$

$$
+ \rho_{im'\sigma im\bar{\sigma}} \hat{f}^\dagger_{im\sigma} \hat{f}_{im'\bar{\sigma}} - \rho_{im'\sigma im\sigma} \hat{f}^\dagger_{im\bar{\sigma}} \hat{f}_{im'\bar{\sigma}} - \rho_{im\bar{\sigma}im\sigma} \hat{f}^\dagger_{im\sigma} \hat{f}_{im'\sigma})
$$

$$
+ \sum_{im\sigma} \epsilon_{im\sigma} \hat{f}^\dagger_{im\sigma} \hat{f}_{im\sigma} - \sum_i \sum_m h_{im} \hat{n}_{im} - \sum_{ii'mm'} \langle \hat{O}^\dagger_{im} \hat{O}_{i'm'} \rangle_s \sum_\sigma t_{imi'm'\sigma} \hat{f}^\dagger_{im\sigma} \hat{f}_{i'm'\sigma}. \tag{23}
$$

We mention that in prior work [21], the spin-flip and pair-hopping terms were argued to be well treated in the slave-particle sector instead. Namely, they were removed from the spinon Hamiltonian and the following terms were added to the spin+orbital-slave Hamiltonian:

$$
- J \sum_{m \neq m'} (\hat{S}^+_{im\uparrow} \hat{S}^-_{im\downarrow} \hat{S}^+_{im'\downarrow} \hat{S}^-_{im'\uparrow} + \hat{S}^+_{im\uparrow} \hat{S}^+_{im\downarrow} \hat{S}^-_{im'\uparrow} \hat{S}^-_{im'\downarrow} + \text{H.c.}) \tag{24}
$$

where the $\hat{S}$ operators in the number basis are

$$
\hat{S}^+ = \begin{pmatrix} 0 & 0 \\ 1 & 0 \end{pmatrix}, \quad \hat{S}^- = \begin{pmatrix} 0 & 1 \\ 0 & 0 \end{pmatrix}. \tag{25}
$$

While such an *ad hoc* approach is not the strictly theoretically consistent way to split operators between the spinon and slave boson sectors, in practice it does reproduce the desired behavior of the spin-flip and pair-hopping terms in the slave-boson sector and does not introduce any numerical difficulties.

Our approach provides some insights into this inconsistency issue while simultaneously easing some technical problems that can arise in the spin+orbital-slave approach. Part of the inconsistency is that the *ad hoc* $\hat{S}^\pm$ slave operators are not the same as the $\hat{O}$ operators (the only way to make them the same is the extreme choice $C_{im\sigma} = 0$). For example, at half-filling when $C_{im\sigma} = 1$, $\hat{O}$ and $\hat{O}^\dagger$ are the same operator and equal the $\hat{S}_x$ Pauli matrix, so one can not use $\hat{O}$ and $\hat{O}^\dagger$ to represent any sensible representation of the spin-flip or pair-hopping interaction terms. If we choose to include some unphysical states, however, things become different. For example, if we widen the range of the spin+orbital slave-boson occupancies from $\{0,1\}$ to $\{-1,0,1,2\}$ then $\hat{O}^\dagger$ and $\hat{O}$ become different. One can then write a more natural interaction term of the form

$$
- J \sum_{m \neq m'} (\hat{O}^\dagger_{im\uparrow} \hat{O}_{im\downarrow} \hat{O}^\dagger_{im'\downarrow} \hat{O}_{im'\uparrow}
$$

$$
+ \hat{O}^\dagger_{im\uparrow} \hat{O}^\dagger_{im\downarrow} \hat{O}_{im'\uparrow} \hat{O}_{im'\downarrow} + \text{H.c.}) \tag{26}
$$

that only uses the slave-boson $\hat{O}$ operators.

Separately, enlarging the set of occupancies beyond $\{0,1\}$ has some technical advantages. When the occupancies are limited to $\{0,1\}$, then we have the analytical form [26] given by $C_{im\sigma} = [n_{im\sigma}(1 - n_{im\sigma})]^{-1/2}$. For occupancies nearing the extremes ($n_{im\sigma} \to 0$ or 1), the $C_{im\sigma}$ become very large, the $O_{im\sigma}$ matrices become ill-behaved, and the numerical algorithm using them becomes difficult to stabilize. Permitting a wider range of occupancies such as $\{-1,0,1,2\}$ makes the $C_{im\sigma}$ have reasonable values and the numerical procedure is well behaved. In the large interaction limit, the addition of the

unphysical states (e.g., occupancies -1 and 2 in this case) is not a major error since number fluctuations are suppressed; the main problem is in the weak interaction regime where this enlargement of the occupancy basis provides numerical stability but can produce quantitative errors.

III. MEAN-FIELD TESTS

We now proceed to describe computational results based on a simple single-site, paramagnetic, nearest-neighbor, mean-field solution of the slave Hamiltonian at half-filling. This will permit us to both reproduce prior literature as well as to compare various slave Hamiltonians to each other.

To do so, we shift the local interaction energies so that they are zero at half-filling, i.e., when $n_{im\sigma} = 1/2$. We also make the standard choice $U' = U - 2J$. The local interaction term (ignoring for the moment the spin-flip and pair-hopping terms) takes the form from prior work [20]:

$$
\hat{H}^i_{\text{int}} = \frac{U - 2J}{2} (\hat{n}_i - n^i_{\text{orb}})^2 + J \sum_m (\hat{n}_{im} - 1)^2
$$

$$
- \frac{J}{2} \sum_\sigma (\hat{n}_{i\sigma} - n^i_{\text{orb}}/2)^2, \tag{27}
$$

where n^i_{orb} is the number of localized correlated spatial orbitals on site i.

In the single-site mean-field approximation, we will be solving for a single-site self-consistently coupled to an averaged bath of bosons on the nearest-neighbor sites. Our assumptions ensure that all sites are identical with no spin polarization. Furthermore, to connect to the literature, we further assume that in the multiorbital case there are only nonzero hoppings between nearest-neighbor orbitals with the same m index. With all these assumptions, it is easy to see that $C_{i\alpha} = 1$ is the choice that gives half-filling for the slave problem at $U = U' = J = 0$. In addition, we can set the Lagrange multipliers $h_{i\alpha} = 0$ since we have set the half-filling energy to be zero. The density matrix elements $\langle \hat{f}^\dagger_{im\sigma} \hat{f}_{i'm'\sigma} \rangle_f$ that renormalize the slave-boson hoppings will be spin and site independent and will be nonzero only when $m = m'$. Hence they can be absorbed into the definition of the hopping elements $t_{imi'm'\sigma}$. The density of states for a spinon band is taken to be the standard semicircular one

$$
D(E) = \begin{cases} c \frac{\sqrt{4t^2 - E^2}}{2\pi t^2} & \text{if } |E| < 2|t| \\ 0 & \text{else} \end{cases}.
$$

We begin with $J = 0$. The slave Hamiltonian is

$$H_s = \frac{U}{2} \sum_i \left(\sum_\alpha \hat{N}_{i\alpha} - n_{\text{orb}} \right)^2$$
$$- \sum_{i\alpha} \sum_{m \in \alpha} \left(\hat{O}_{i\alpha} t_m^{\text{eff}} + \hat{O}_{i\alpha}^\dagger t_m^{\text{eff}} \right), \quad (28)$$

where the effective hoping for spatial orbital m is

$$t_m^{\text{eff}} = \sum_{i'\alpha'} \sum_{m'\sigma \in \alpha'} t_{imi'm'\sigma} \langle \hat{O}_{\alpha'} \rangle_s. \quad (29)$$

The simple form of this Hamiltonian makes it easy to directly read off the quasiparticle weight renormalization Z_α, which narrows the spinon bands:

$$Z_\alpha = \langle \hat{O}_\alpha \rangle_s^2. \quad (30)$$

When $Z_\alpha = 0$, a Mott insulator is realized in such a simple single-site model [27]. We solve the problem self-consistently for different slave models. Since at half-filling the Lagrange multipliers $h_{i\alpha} = 0$, all that is required to solve the spinon problem is to renormalize each spinon bandwidth (i.e., hopping) by the appropriate Z_α factor.

A. Single-band Mott transition

We begin with a single-band model where there is one spatial orbital per site. Figure 1 compares various slave models based on the dependence of Z on U. Specifically, we compare the slave-rotor model (allowed occupancies from $-\infty$ to $+\infty$), the orbital slave model (allowed occupancies 0, 1, or
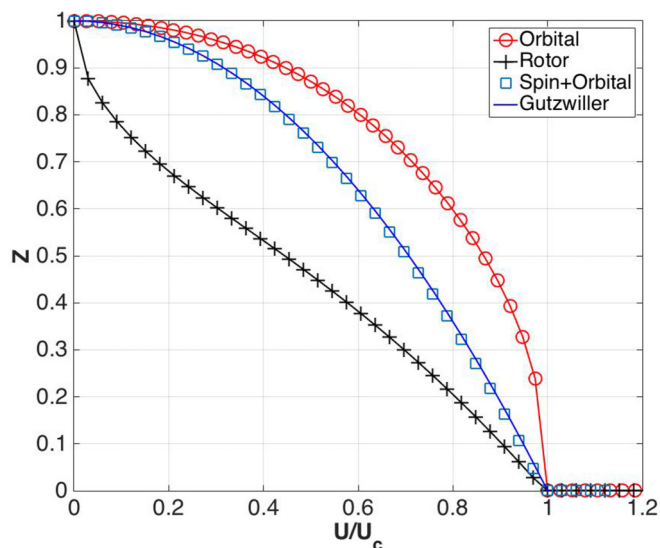

FIG. 1. (Color online) Quasiparticle weight Z as a function of U/U_c for different slave-particle models for the paramagnetic single-band Hubbard at half-filling. U_c is the critical value of U when $Z = 0$, i.e., the Mott transition, for each model. The black squares show slave-rotor results, the blue line is the Gutzwiller approximation results which for this model are the same as the spin+orbital-slave ("slave-spin") results in blue squares, and the red circles show the orbital-slave results (identical to the number slave). We note that the orbital-slave Hilbert space is very small, so that it does not agree with the rotor, unlike the two-band slave number.

2) which here is identical to the number-slave model, the spin+orbital-slave ("slave-spin") model (allowed occupancies 0 or 1) and the Gutzwiller approximation where $Z_{\text{Gutzwiller}} = 1 - (U/U_c)^2$.

For this system, the Gutzwiller and spin+orbital-slave methods predict exactly the same results, as noted previously [20]. In fact, the spin+orbital-slave model, at half-filling for a single orbital per site at the single-site mean-field level, can be shown to be isomorphic to the Gutzwiller approximation as well as to the Kotliar-Ruckenstein model as described by Bunemann [16]. This shows that, beyond their utility as mathematical models, such slave-boson methods can parallel and help understand other approaches that originate from apparently different sets of many-body approximations.

The slave-rotor method has an aberrant behavior for small U. Specifically, Z for the slave-rotor method has the small U expansion

$$Z_{\text{rotor}} = 1 - O(\sqrt{U/t_{\text{eff}}}). \quad (31)$$

The reason for this behavior is due to the unbounded number states permitted in the slave-rotor model. Specifically, in the number basis the slave-rotor problem corresponds to an infinite one dimensional lattice labeled by N_i, with hoppings t^{eff} between neighboring sites, and with a quadratic potential $UN_i^2/2$. For small U, the ground state of this problem will be spread over many sites so that we can take the continuum limit. The problem turns into the textbook one-dimensional harmonic oscillator with mass $1/(2t_{\text{eff}})$ and spring constant U. The ground-state wave function $\psi(N_i)$ is a Gaussian, and $\langle O \rangle_s = \sum_n \psi(n)\psi(n-1)$ can be computed. Expansion in U then gives the above form.

In reality, however, perturbation theory guarantees that quasiparticle weights are modified starting at second order in the interaction strength:

$$Z = 1 - O(U^2/t_{\text{eff}}^2). \quad (32)$$

The slave rotor fails since for small U it spreads the wave function over a large number of unphysical states. What this means is that one would incorrectly overestimate the importance of electronic correlations at weak interaction strengths when using the slave-rotor method. In this view, our orbital and number-slave methods may be viewed as corrected rotors which are restricted to the appropriate finite set of physical states. Finally, Fig. 1 illustrates that slave methods employing finite slave Hilbert spaces all automatically correct the small U behavior.

B. Isotropic two-band Mott transition

Next, we consider a two-band degenerate Hubbard model. Figure 2 displays the results. We note that the two band e_g model is of physical relevance as the slave rotor has shown itself to be of use in e_g nickelate systems within a pd model [19]. For this particular degenerate case with high symmetry, the spin-slave and orbital-slave models turn out to be identical since each posits two slave particles each with the allowed occupations 0, 1, or 2. We note that, in this case, the slave rotor and number slave become very similar for large U: once slave number fluctuations of N_i are small, the size of the slave Hilbert space becomes irrelevant.
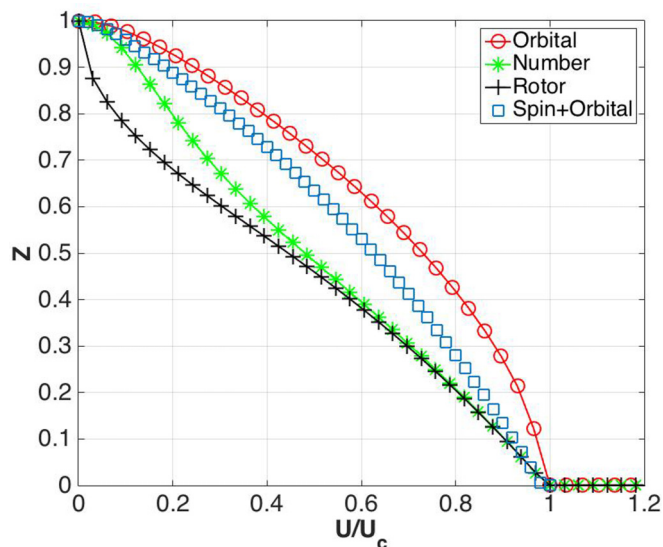
FIG. 2. (Color online) Quasiparticle weight Z as a function of U/U_c for different slave-particle models for a degenerate paramagnetic two-band Hubbard model at half-filling.

C. Anisotropic orbital-selective Mott transition

We present mean-field calculations exemplifying the orbital-selective Mott transition in an anisotropic two band model with paramagnetic solution and at half-filling. We take spatial orbital $m = 1$ to have the larger hopping t_1 while $m = 2$ has the smaller hopping t_2. Hence, t_2/t_1 specifies the degree of anisotropy.

The first slave model for this system is the spin+orbital method, which has been used previously [20,21]: each slave boson has allowed occupancies 0 or 1. The second model is to forgo the explicit spin degree of freedom in the slave description and to employ the orbital slave model where each slave boson has allowed occupancies 0, 1, and 2. The comparison tests the importance of explicit treatment of spin in the electronic correlations for such a system. We will focus on the orbital-selective Mott transition (OSMT) when one orbital has a finite bandwidth and is metallic while the other has undergone a Mott insulating transition and is localized.

We begin with $J = 0$. Figure 3 illustrates the behavior of the renormalization factor Z for both bands versus U for three different t_2/t_1 ratios within the two slave particle models. An OSMT occurs for small enough t_2/t_1 ratio but the critical value depends on the type of slave model. For the orbital-slave model, we find that OSMT occurs when $t_2/t_1 < 0.25$, while for spin+orbital slave, we must have a slightly smaller value of $t_2/t_1 < 0.2$.

We now consider $J > 0$. We continue to treat the spinon problem as that of a simple, paramagnetic, half-filled tight-binding model with two separate bands with each hopping renormalized by the appropriate $\langle \hat{O}_\alpha \rangle_s$. For the orbital-slave model, we can only include the first two terms of Eq. (27) due to the lack of an explicit spin label in the slave description. Thus we will compare the orbital slave and spin+orbital slave using the same interaction term

$$\hat{H}_{\text{int}}^i = \frac{U - 2J}{2}(\hat{N}_i - 2)^2 + J \sum_m (\hat{N}_{im} - 1)^2. \quad (33)$$
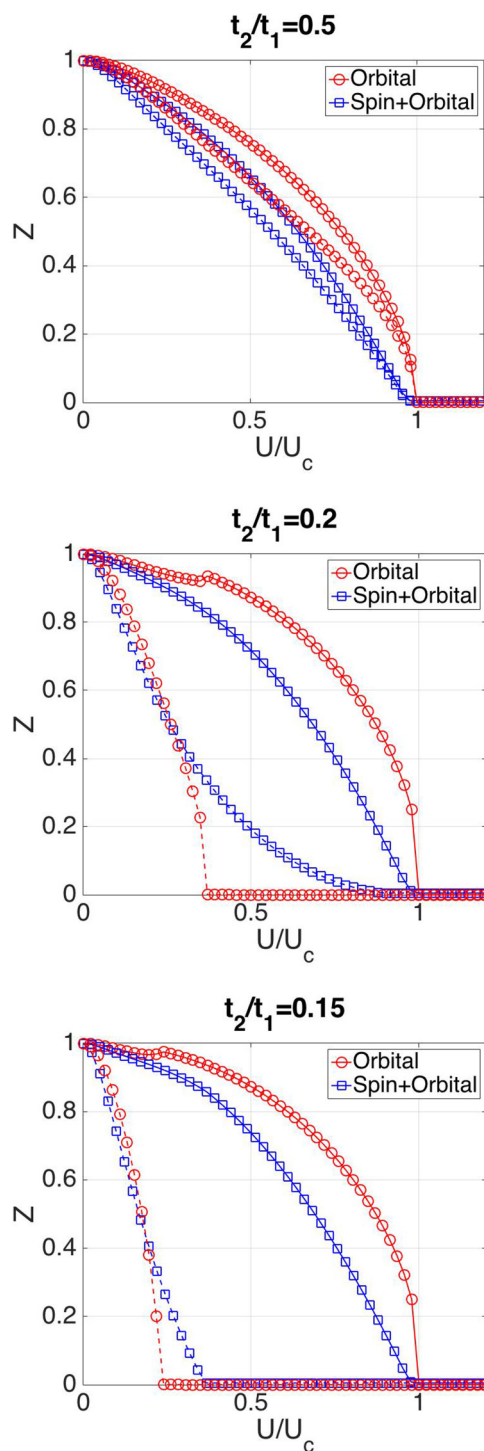

FIG. 3. (Color online) Quasiparticle weights for the paramagnetic anisotropic two-band single-site Hubbard model at half-filling as predicted by the orbital+spin-slave model (blue squares) and the orbital-slave model (red circles) at $J = 0$ for three t_2/t_1 ratios. In each plot, the Z value for the first orbital with larger hopping t_1 is denoted by symbols and a continuous line while for the second orbital symbols and a dashed line are used. An OSMT occurs when the two Z do not go to zero at the same U value: orbital slave (red circles) in the center plot and both slave models in the lower plot.

It is clear from the above two interaction terms that, for fixed U, $J > 0$ permits larger orbital independent number fluctuations
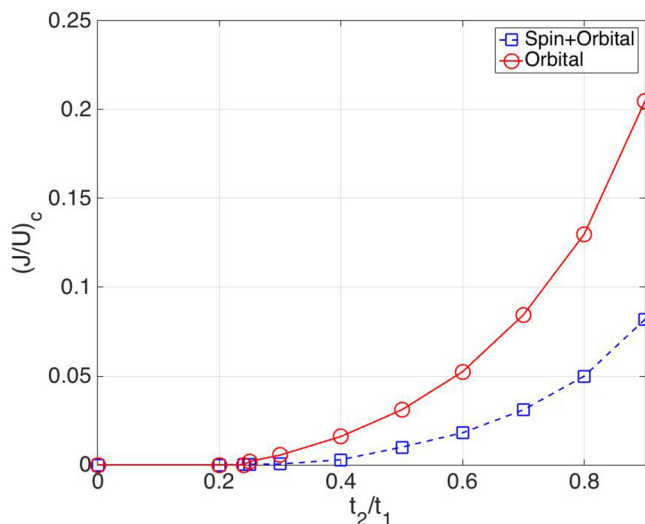
FIG. 4. (Color online) Phase diagram for the anisotropic two-band single-site Hubbard model at half-filling as a function of the anisotropy ratio t_2/t_1 and J. Two slave-boson methods are used: orbital slave (red circles) and spin+orbital slave (blue squares). In each case, the boundary curve demarcates the possible existence of an orbital-selective Mott Transition when U is ramped up from $U = 0$. Regions above the boundary display OSMT, while regions below it present a standard Mott transition where both bands become insulating at the same critical U_c value.

(i.e., it reduces the correlation effect of this mode) since $U' = U - 2J$ becomes smaller in the first term. However, the second $+J$ term simultaneously punishes intra-orbital number fluctuations and thus enhances intra-orbital correlation effects which in turn favors an OSMT.

The phase diagram as a function of t_2/t_1 and J for this system in shown in Fig. 4. The boundaries shown separate regions where OSMT occurs (above the boundaries) from where a standard Mott transition occurs (below the boundaries). The figure confirms the fact that increasing J favors OSMT. Qualitatively, the orbital slave and spin+orbital slave show very similar behavior: they have a critical t_2/t_1 at $J = 0$ between $0.2 - 0.25$ for OSMT to occur, and then with increasing J the critical t_2/t_1 becomes larger so less anisotropy is needed to drive an OSMT, as observed previously in DMFT [28] and spin+orbital slave calculations [20].

We have also considered the case where we permit the orbital-slave model to have unlimited occupations: namely, we have a two rotor model (one for each orbital occupation). In this case, we find that no OSMT is possible when $J = 0$ for any bandwidth ratio t_2/t_1. This result is similar to previous DMFT [20,28], which found that a finite J is needed in order to have an OSMT. However, it disagrees with the results of previous orbital+spin-slave results [20] as well as our results above where we find that a small enough bandwidth ratio t_2/t_1 makes an OSMT possible even for $J = 0$. These differences further illustrate the need for multiple models and cross verification when describing a possible OSMT for real materials which have complex band structures (e.g., the three-band $Ca_{2-x}Sr_xRuO_4$ system [3]).

Prior work [20] has shown that the presence of the Hund's term

$$-\frac{J}{2}\sum_\sigma \sum_{m\neq m'} (\hat{n}_{m\sigma} - 1/2)(\hat{n}_{m'\sigma} - 1/2) = -\frac{J}{2}\sum_\sigma (\hat{n}_{i\sigma} - 1)^2 \tag{34}$$

makes OSMT slightly more difficult to achieve as it increases interorbital $m \neq m'$ correlations by favoring spin pairing between different orbitals but does not aid intraorbital correlations. Separately, adding the spin-flip and pair-hopping terms makes OSMT easier to achieve [20].

Although not directly relevant to our main focus, for completeness we include a final comparison based on a fixed slave model with various combination of interaction terms. We choose the spin+orbital orbital model and then choose to include different interaction terms in the slave-particle Hamiltonian. The first choice is the interaction terms used above in Eq. (33). The second choice is to add the Hund's term

$$\hat{H}_{int}^i = \frac{U - 2J}{2}\big(\hat{N}_i - n_{orb}^i\big)^2 + J\sum_m (\hat{N}_{im} - 1)^2$$
$$- \frac{J}{2}\sum_\sigma (\hat{N}_{i\sigma} - 1)^2. \tag{35}$$

Prior work [20] has shown that the presence of the Hund's term makes OSMT more difficult to achieve as it increases interorbital correlations by favoring spin-pairing among different orbitals but does not enhance intraorbital correlations.

The third choice is to add the spin-flip and pair-hopping terms as per the *ad hoc* method of Eq. (24):

$$\hat{H}_{int}^i = \frac{U - 2J}{2}(\hat{N}_i - 2)^2 + J\sum_m (\hat{N}_{im} - 1)^2$$
$$- \frac{J}{2}\sum_\sigma (\hat{N}_{i\sigma} - 1)^2$$
$$- J\sum_{m\neq m'} (\hat{S}_{im\uparrow}^+ \hat{S}_{im\downarrow}^- \hat{S}_{im'\downarrow}^+ \hat{S}_{im'\uparrow}^-$$
$$+ \hat{S}_{im\uparrow}^+ \hat{S}_{im\downarrow}^+ \hat{S}_{im'\uparrow}^- \hat{S}_{im'\downarrow}^- + \text{H.c.}). \tag{36}$$

Adding these spin-flip and pair-hopping terms makes OSMT easier to achieve [20].

Phase diagrams for the second and third choices above are available in the literature [20] and are reproduced in Fig. 5, which also includes the results of the first choice as well. We note that only including the intraorbital terms (first choice) or all terms (third choice) leads to essentially the same phase diagram. However, excluding the spin-flip and pair-hopping terms (second choice) makes it harder to achieve an OSMT phase: one can not achieve an OSMT for any reasonable J once the bandwidth ratio t_2/t_1 exceeds ≈ 0.6. The physics behind this progression is as follows. Starting with $J = 0$ and a relatively large U, the ground-state basically contains only states that are half-filled and have a total of two electrons per site (there are six such states). Adding the intraorbital term (first choice) with $J > 0$ then further restricts us to the four states with only one electron per orbital (but with no preference for spin states). Such a ground state can suffer an OSMT
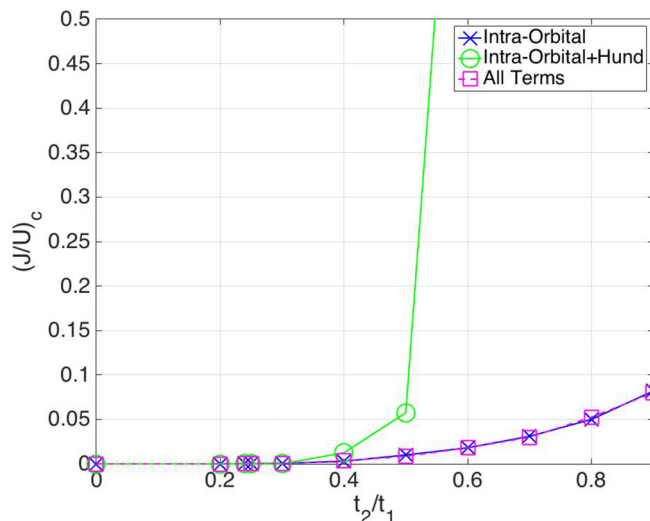
FIG. 5. (Color online) Phase diagram for the anisotropic two-band single-site Hubbard model at half-filling as a function of the anisotropy ratio t_2/t_1 and J for the spin+orbital-slave model. Three different interaction terms are used: intraorbital term only [Eq. (33)], intraorbital plus Hund's [Eq. (35)], and all terms included [Eq. (36)].

when further increasing U since the narrower band (more localized orbital) can become fully localized. Next, adding the Hund's term (second choice) creates a preference for the two spin-aligned states in this four dimensional subspace by lowering their energy: this enhances interorbital correlations at the expense of intraorbital correlations which favor an OSMT phase. Third, adding the spin-flip and pair-hopping (third choice) terms essentially cancels the effect of the Hund's term. This is explained by a straightforward computation of the matrix elements of this interaction in the four dimensional subspace. One finds that the spin-flip term couples the two states where electrons have opposite spins with a strength that is precisely such that their symmetric combination has the same energy lowering as the Hund's term induces for the spin-aligned states. Thus we are essentially back to the four states we had when only operating with the intraorbital interaction (first choice). Our final comment is that these differences are not very dramatic once the hopping ratio t_2/t_1 is below ≈ 0.5. As Fig. 5 shows, in all cases only a modest value for J is sufficient to stabilize the OSMT phase instead of a standard Mott transition.

D. Ground-state energies

A final and most stringent test for the slave models is to compare their total energies. In the interest of space, we will focus on the simplest case of degenerate orbitals, isotropic hopping, and phases that are paramagnetic and paraorbital (no orbital differentiation) to make some general comments. In a fully self-consistent model with more parameters and nondegenerate bands, we may expect more complexity to be revealed. Previous work [29] has shown that ground-state calculations can reveal competition between the orbital-selective Mott state (due to very large crystal-field splitting) and an antiferromagnetic Mott insulating state (due to a large J), a transition which is likely first order [29].
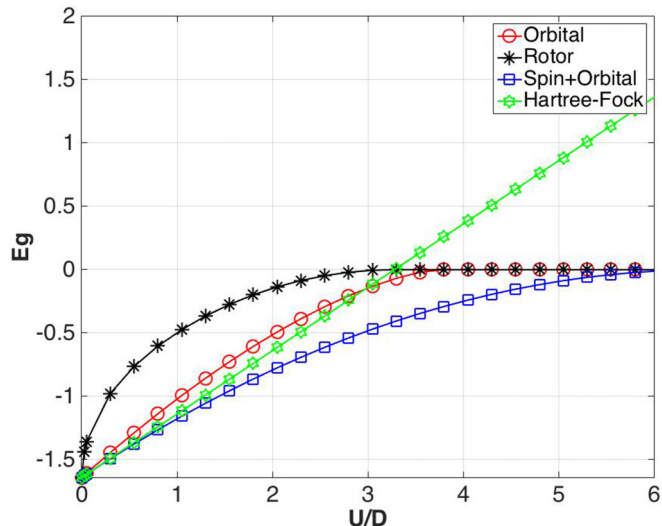

FIG. 6. (Color online) Ground-state energy per site (E_g/t) of a single-band Hubbard model at $J = 0$ in the paramagnetic phase at half-filling for a variety of slave representations as well as for the Hartree-Fock approximation. $D = 2t$ is the band width of the noninteracting system. For this model, the orbital slave is identical to the number slave and the spin slave is the same as the spin+orbital slave.

With $J = 0$, the ground-state energy per site of the paramagnetic and paraorbital phase is

$$E_g = -\sum_{\alpha} \sum_{m \in \alpha} t_m^{\text{eff}} \langle \hat{O}_\alpha \rangle_s + \frac{U}{2} \left\langle \left[\sum_{\alpha} \hat{N}_\alpha - n_{\text{orb}} \right]^2 \right\rangle. \quad (37)$$

We compute the ground-state energy as a function of U for one-band and two-band isotropic models at half-filling (same systems that are in the above sections) and also include the Hartree-Fock total energy. Figures 6 and 7 display the energies versus U for the one-band and two-band cases, respectively. The plots employ the half-band width $D = 2t$.
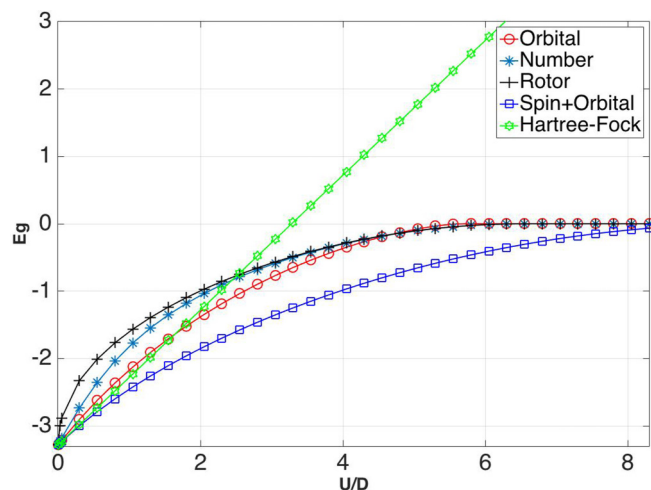

FIG. 7. (Color online) Ground-state energy per site (E_g/t) for an isotropic two-band Hubbard model at half-filling for $J = 0$ in the paramagnetic and paraorbital phase.

In all cases, for large enough U, the slave models produce an insulating phase (i.e., isolated atomic-like sites), which has zero hopping and zero number fluctuation and thus zero energy in this model. The Hartree-Fock total energy necessarily has a linear dependence on U for the high degree of spin and orbital symmetry since the Hartree-Fock Slater determinant wave function will be unchanged versus U and always predicts a metallic system.

The next observation is that for small U, some of the slave models do worse than Hartree-Fock. However, as U is increased their total energies eventually drop below the Hartree-Fock one. Furthermore, increasing the number of bands from one to two improves the total energies of all slave methods compared to Hartree-Fock. For a given number of bands, increasing the fine-grainedness of the slave model (i.e., having more slave modes per site) also lowers the total energy. Hence the slave-rotor is generally the worst performer.

A final observation is that only the fully fine-grained spin+orbital-slave method always predicts a total energy below that of Hartree-Fock. It also has the correct linear slope of E_g versus U matching the Hartree-Fock one. The other slave methods have higher slopes of E_g versus U at the origin so that they can only outperform Hartree-Fock beyond some finite value of U. The slope matching of the spin+orbital slave is a natural expression of its accounting in detail for all the quantum numbers on each site and in being forced (like all slave models) to reproduce the noninteracting state at $U = 0$. The fact that the other slave models have higher slopes is a reflection of their larger (and quantitatively incorrect) number fluctuations at $U = 0$. Namely, the interaction Hamiltonian $\hat{H}^{\text{int}}$ is a quadratic function of the occupancy numbers so that its expectation value (the interaction energy) depends directly on the fluctuations of these occupancies; at fixed U, the larger the set of allowed occupancies in a slave model, the larger this quadratic fluctuation and the higher the interaction energy. In fact, the number fluctuations of the slave-rotor model are so large at $U = 0$ that they lead to a pathological infinite slope of E_g versus U at $U = 0$. By comparison, the number-slave method, which can be viewed as a corrected rotor, has a much more reasonable behavior.

As a side note, it is interesting that for the single-band case, one has the following analytical results based on the coincidence of the of the spin+orbital-slave and Gutzwiller approximations. In the metallic phase, where $U < U_c$, the quasiparticle weight Z is given by

$$Z = 1 - U^2/U_c^2 \tag{38}$$

and from perturbation theory at small Z [18],

$$U_c = 8D. \tag{39}$$

Using the definition

$$t_0 = t \langle f_{im\sigma}^\dagger f_{im\sigma} \rangle_{U=0}, \tag{40}$$

the ground-state energy is given by

$$E_g = -2t_0 + \frac{U}{4} - \frac{U^2}{128 t_0^2}. \tag{41}$$

For the insulating state ($U \geqslant U_c$), we have $E_g = 0$.

Our calculations in this section permit us to say that while our generalized approach permits us to easily compare different slave models and isolate different degrees of freedom simply, total energy comparisons are much more challenging. First, one should do energy comparisons of different phases within a single slave model since the differing models can produce differing total energies with dependence on the details of the system. Second, after understanding the relevant degrees of freedom and how they influence the physical behavior, the total energy calculation should be most accurate with the most fine-grained model, which is in the spin+orbital-slave representation ("slave spin" in the literature).

IV. CONCLUSIONS

We have developed a generalized formalism that reproduces previous slave-particle formalisms in appropriate limits but also allows us to define and explore intermediate models and to compare them systematically. Our formalism moves beyond the analogy with angular momentum behind the slave-rotor formalism, and instead works directly in the physically correct finite-sized number representation permitting new models to be developed in a more natural way. As an example, we have shown how the standard Mott transition as well as the orbital selective Mott transition appear in different slave models for single-band and two-band Hubbard models.

We believe it is useful to have a variety of slave-particle methods on hand as they provide computationally inexpensive methods for exploring the role of electronic correlations in materials and interfaces with broken symmetries (e.g., orbital symmetry breaking). The cheap computational load is particularly advantageous for interfacial systems where translational symmetry is lost in one direction and simulation cells that capture the region near the interface must contain at least tens to hundreds of atoms. As such, these simpler slave-particle models are useful for exploratory research where more accurate and expensive Hubbard-model solvers such as DMFT [4,30] would be prohibitive to apply routinely. The ability to isolate potentially interesting correlated degrees of freedom from each other by choosing different slave approaches may illuminate which degrees of freedom are the most critical to model accurately.

APPENDIX

In this appendix, we provide some detailed examples of how the physical subspace is isolated from the extended Hilbert space of spinon+slave-boson states and how the operators act in the physical subspace. In the process, we also provide explicit examples for various choices of the slave labels α. We focus on a single site i and hence suppress the site label i below.

The original Hilbert space, i.e., the Fock space of the fermionic $\hat{d}_{m\sigma}$ field operators, is spanned by basis kets in the occupancy number representation for the field operators and have the form $|\{n_{m\sigma}\}\rangle$ where $n_{m\sigma} \in \{0, 1\}$. The enlarged Hilbert space for spinons and slave particles is spanned by

product kets in the number occupancy basis of the form

$$|\{n_{m\sigma}\}\rangle_f |\{N_\alpha\}\rangle_s,$$

where, again, $n_{m\sigma} \in \{0,1\}$ are the fermionic spinon occupancies, while N_α are the bosonic particle counts. The f and s subscripts label the spinon and slave-boson kets.

The constraint of Eq. (6) on the physical allowed states translates to the numerical constraint

$$N_\alpha = \sum_{m\sigma \in \alpha} n_{m\sigma}. \qquad (A1)$$

We remember that we choose the $\{n_{m\sigma}\}$ to match exactly between the original electron and spinon kets.

We begin with the simplest example of a single spatial orbital on the site where the kets look like $|n_\uparrow, n_\downarrow\rangle_f |\{N_\alpha\}\rangle_s$. There are two states for electrons and thus a total of four possible configurations: no electrons, one spin-up electron, one spin-down electron, and a pair of spin-up and spin-down electrons. If we have a single slave boson per site to simply count the number of electrons so the α label is nil (i.e., the number-slave representation), then our four physically allowed kets are

$$|0,0\rangle_f |0\rangle_s, \ |1,0\rangle_f |1\rangle_s, \ |0,1\rangle_f |1\rangle_s, \ |1,1\rangle_f |2\rangle_s.$$

We note that the number of slave particles is constrained by Eq. (6) to the total number of spinons.

Next, if we have this single orbital but instead we choose to have a slave mode per spin channel (i.e., the spin+orbital-slave representation), then we have two sets of slave bosons since now $\alpha = \sigma$. The four physical states are now

$$|0,0\rangle_f |0,0\rangle_s, \ |1,0\rangle_f |1,0\rangle_s, \ |0,1\rangle_f |0,1\rangle_s, \ |1,1\rangle_f |1,1\rangle_s.$$

A more complex set of examples has two spatial orbitals per site. Here, we have four choices of spinon label $m\sigma$ which we order as $1\uparrow, 1\downarrow, 2\uparrow, 2\downarrow$. For the number-slave representation, we have the 16 physical kets

$$|0,0,0,0\rangle_f |0\rangle_s, \ |1,0,0,0\rangle_f |1\rangle_s, \ |0,1,0,0\rangle_f |1\rangle_s,$$
$$|0,0,1,0\rangle_f |1\rangle_s, \ |0,0,0,1\rangle_f |1\rangle_s, \ |1,1,0,0\rangle_f |2\rangle_s,$$
$$|1,0,1,0\rangle_f |2\rangle_s, \ |1,0,0,1\rangle_f |2\rangle_s, \ |0,1,1,0\rangle_f |2\rangle_s,$$
$$|0,1,0,1\rangle_f |2\rangle_s, \ |0,0,1,1\rangle_f |2\rangle_s, \ |1,1,1,0\rangle_f |3\rangle_s,$$
$$|1,1,0,1\rangle_f |3\rangle_s, \ |1,0,1,1\rangle_f |3\rangle_s, \ |0,1,1,1\rangle_f |3\rangle_s,$$
$$|1,1,1,1\rangle_f |4\rangle_s.$$

An orbital-slave representation has slave bosons counting the number of electrons in each spatial orbital, so $\alpha = m$. The 16 allowed kets are

$$|0,0,0,0\rangle_f |0,0\rangle_s, \ |1,0,0,0\rangle_f |1,0\rangle_s, \ |0,1,0,0\rangle_f |1,0\rangle_s,$$
$$|0,0,1,0\rangle_f |0,1\rangle_s, \ |0,0,0,1\rangle_f |0,1\rangle_s, \ |1,1,0,0\rangle_f |2,0\rangle_s,$$
$$|1,0,1,0\rangle_f |1,1\rangle_s, \ |1,0,0,1\rangle_f |1,1\rangle_s, \ |0,1,1,0\rangle_f |1,1\rangle_s,$$
$$|0,1,0,1\rangle_f |1,1\rangle_s, \ |0,0,1,1\rangle_f |0,2\rangle_s, \ |1,1,1,0\rangle_f |2,1\rangle_s,$$
$$|1,1,0,1\rangle_f |2,1\rangle_s, \ |1,0,1,1\rangle_f |1,2\rangle_s, \ |0,1,1,1\rangle_f |1,2\rangle_s,$$
$$|1,1,1,1\rangle_f |2,2\rangle_s.$$

Alternatively, one can use the spin-slave representation where the bosons count the number of electrons of each spin, so $\alpha = \sigma$. The allowed kets are

$$|0,0,0,0\rangle_f |0,0\rangle_s, \ |1,0,0,0\rangle_f |1,0\rangle_s, \ |0,1,0,0\rangle_f |0,1\rangle_s,$$
$$|0,0,1,0\rangle_f |1,0\rangle_s, \ |0,0,0,1\rangle_f |0,1\rangle_s, \ |1,1,0,0\rangle_f |1,1\rangle_s,$$
$$|1,0,1,0\rangle_f |2,0\rangle_s, \ |1,0,0,1\rangle_f |1,1\rangle_s, \ |0,1,1,0\rangle_f |1,1\rangle_s,$$
$$|0,1,0,1\rangle_f |0,2\rangle_s, \ |0,0,1,1\rangle_f |1,1\rangle_s, \ |1,1,1,0\rangle_f |2,1\rangle_s,$$
$$|1,1,0,1\rangle_f |1,2\rangle_s, \ |1,0,1,1\rangle_f |2,1\rangle_s, \ |0,1,1,1\rangle_f |1,2\rangle_s,$$
$$|1,1,1,1\rangle_f |2,2\rangle_s.$$

The final point is to check that the original electron operators $\hat{d}_{m\sigma}$ have the same effect as the combination of spinon and slave $\hat{f}_{m\sigma} \hat{O}_\alpha$ in the physical subspace. That this is in fact true follows directly from the defining Eqs. (7)–(9) along with the constraint on N_α in Eq. (A1). It is easy to check that the matrix elements of $\hat{d}_{m\sigma}$ and $\hat{f}_{m\sigma} \hat{O}_\alpha$ must match:

$$\langle n'_{m\sigma} | \hat{d}_{m\sigma} | n_{m\sigma} \rangle = {}_f\langle n'_{m\sigma} | \hat{f}_{m\sigma} | n_{m\sigma} \rangle_f \cdot {}_s\langle N'_\alpha | \hat{O}_\alpha | N_\alpha \rangle_s.$$

The matching of the $\hat{d}$ and $\hat{f}$ matrix elements is clear because the occupancies $n_{m\sigma}$ and $n'_{m\sigma}$ match by definition on both sides and both operators have identical behavior on the occupancies as per Eqs. (7) and (8). Thus both sides are nonzero only if the n' occupancy set has one fewer total count than the n occupancy set. As long as $N_\alpha > 0$, the matrix element of $\hat{O}_\alpha$ is unity because $N'_\alpha = N_\alpha - 1$ must be true due to the occupancy matching of Eq. (A1). If $N_\alpha = 0$, it must be that $n_{m\sigma} = 0$, so that the matrix element of $\hat{O}_\alpha$ is irrelevant because the fermionic matrix elements (of $\hat{d}$ and $\hat{f}$) are both zero.

---

[1] M. Imada, A. Fujimori, and Y. Tokura, Rev. Mod. Phys. **70**, 1039 (1998).

[2] S. Nakatsuji and Y. Maeno, Phys. Rev. Lett. **84**, 2666 (2000).

[3] V. I. Anisimov, I. A. Nekrasov, D. E. Kondakov, T. M. Rice, and M. Sigrist, Eur. Phys. J. B **25**, 191 (2002).

[4] A. Georges, G. Kotliar, W. Krauth, and M. Rozenberg, Rev. Mod. Phys. **68**, 13 (1996).

[5] G. Kotliar and D. Vollhardt, Phys. Today **57**, 53 (2004).

[6] S. E. Barnes, J. Phys. F **6**, 1375 (1976).

[7] S. Barnes, J. Phys. F **7**, 12 (1977).

[8] P. Coleman, Phys. Rev. B **29**, 3035 (1984).

[9] N. Read and D. M. Newns, J. Phys. C: Solid State Phys. **16**, L1055 (1983).

[10] N. Read, J. Phys. C: Solid State Phys. **18**, 2651 (1985).

[11] G. Kotliar and A. E. Ruckenstein, Phys. Rev. Lett. **57**, 1362 (1986).

[12] P. A. Lee, N. Nagaosa, and X. G. Wen, Rev. Mod. Phys. **78**, 17 (2006).

[13] M. Raczkowski, R. Fresard, and A. M. Oles, Europhys. Lett. **76**, 128 (2006).

[14] R. Fresard and G. Kotliar, Phys. Rev. B **56**, 12909 (1997).

[15] F. Lechermann, A. Georges, G. Kotliar, and O. Parcollet, Phys. Rev. B **76**, 155102 (2007).

[16] J. Bünemann, Phys. Status Solidi Basic Res. **248**, 203 (2011).

[17] S. Florens and A. Georges, Phys. Rev. B **66**, 165111 (2002).

[18] S. Florens and A. Georges, Phys. Rev. B **70**, 035114 (2004).

[19] B. Lau and A. J. Millis, Phys. Rev. Lett. **110**, 126404 (2013).

[20] L. de'Medici, A. Georges, and S. Biermann, Phys. Rev. B **72**, 205124 (2005).

[21] S. R. Hassan and L. de' Medici, Phys. Rev. B **81**, 035106 (2010).

[22] L. de' Medici, G. Giovannetti, and M. Capone, Phys. Rev. Lett. **112**, 177001 (2014).

[23] J. Kanamori, Prog. Theor. Phys. **30**, 275 (1963).

[24] J. Bünemann, F. Gebhard, and W. Weber, J. Phys.: Condens. Matter **9**, 7343 (1997).

[25] E. Zhao and A. Paramekanti, Phys. Rev. B **76**, 195101 (2007).

[26] M. Z. Hasan and C. L. Kane, Rev. Mod. Phys. **82**, 3045 (2010).

[27] W. F. Brinkman and T. M. Rice, Phys. Rev. B **2**, 4302 (1970).

[28] A. Koga, N. Kawakami, T. M. Rice, and M. Sigrist, Phys. Rev. Lett. **92**, 216402 (2004).

[29] Y. M. Quan, L. J. Zou, D. Y. Liu, and H. Q. Lin, Eur. Phys. J. B **85**, 1 (2012).

[30] G. Kotliar, S. Y. Savrasov, K. Haule, V. S. Oudovenko, O. Parcollet, and C. A. Marianetti, Rev. Mod. Phys. **78**, 865 (2006).